65

NIOBIUM TRISELENIDE: A UNIQUE RECHARGEABLE POSITIVE ELECTRODE MATERIAL

F. A. TRUMBORE

AT&T Bell Laboratories, 600 Mountain Avenue, Murray Hill, NJ 07974 (U.S.A.)

Summary

Niobium triselenide, $NbSe_3$, is a metallically-conducting, fibrous material which can be used directly as a positive electrode material in lithium rechargeable cells. Without any binder or conducting additives, $Li/NbSe_3$ cells have particularly attractive energy and power densities. This paper deals with the performance of $NbSe_3$ positive electrodes for coin and jellyroll cell configurations. Some of the problems related to the attainment of a practical $Li/NbSe_3$ rechargeable battery are considered.

Introduction

A number of fibrous transition metal trichalcogenides are capable of intercalating three lithiums per chalcogenide molecule when used as cathode (positive electrode) materials in lithium nonaqueous cells [1, 2]. Two of these compounds, the tantalum and niobium triselenides, are metallically conducting. Of these two compounds, only the niobium triselenide has been pursued extensively with regard to its electrochemical properties. The fibrous morphology of $NbSe_3$ is shown in Fig. 1, which illustrates the range of fiber sizes and the large surface area of this material. In general, the fibers have a ribbonlike morphology, with the thickness of the ribbons varying such that some ribbons are virtually transparent in the SEM (Fig. 1(b)) while others have a more bulky, slablike morphology as in Fig. 1(c). The insertion and the removal of the lithium has been shown to be highly reversible in $NbSe_3$, which maintains this fibrous morphology, even after extensive charge–discharge cycling in $Li/NbSe_3$ cells [3]. This high degree of reversibility of $NbSe_3$ made it useful for us as a standard cathode material in studies aimed at improving the cycleability of the lithium anode in secondary lithium cells [4].

As these studies progressed, we concluded that $NbSe_3$ was worthy of consideration as a practical cathode material. With a morphology somewhat similar to "Velcro" and a metallic conductivity, the need for either binders or conducting additives is eliminated. Furthermore, the large surface area of the fibers results in easy access of the electrolyte solution and a surprisingly
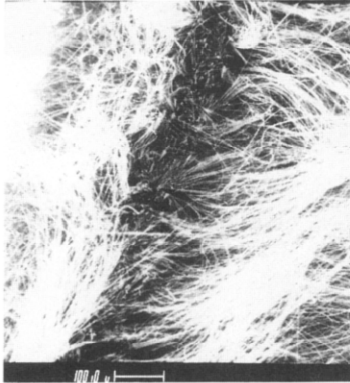
(a)
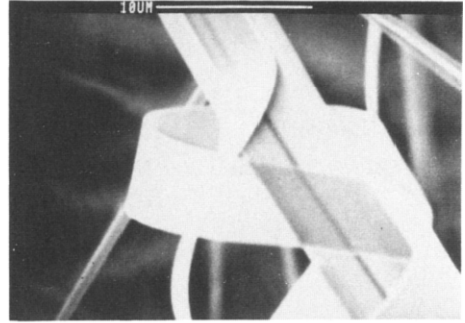
(b)
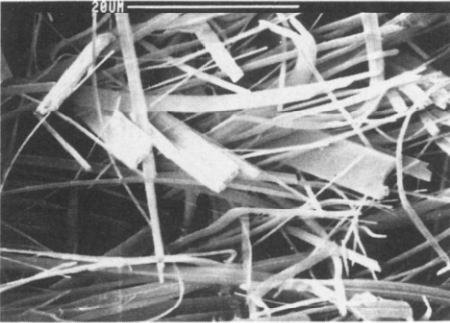
(c)

Fig. 1. (a) Scanning electron microscope (SEM) photograph showing the fibrous morphology of NbSe₃. (b) SEM photograph at higher magnification showing a very thin, "transparent" ribbon curving over and under another ribbon. (c) SEM photograph showing thicker, more bulky fiber morphologies.

high rate capability. In addition, a mid-discharge voltage in the vicinity of 2 V (discussed below), and a high volumetric energy density, make the $Li/NbSe_3$ couple attractive as a high energy density rechargeable system.

Consequently, we initiated an effort at AT&T Bell Labs to develop a rechargeable $Li/NbSe_3$ coin cell for semiconductor memory maintenance applications. After considerable progress, this effort was abandoned with the increasing use of low current CMOS memory devices, which could be serviced adequately by lithium primary batteries. There followed a second, ongoing effort (our "Faraday" project) to develop a high energy density, high rate AA-size, cylindrical, secondary lithium cell for portable applications. The performance of the $Li/NbSe_3$ system in both the coin and cylindrical cells is the subject of this paper.

Coin cells

Some results on our earliest coin cells, with capacities of only 63 mA h, were presented elsewhere [5]. However, the features of the $Li/NbSe_3$
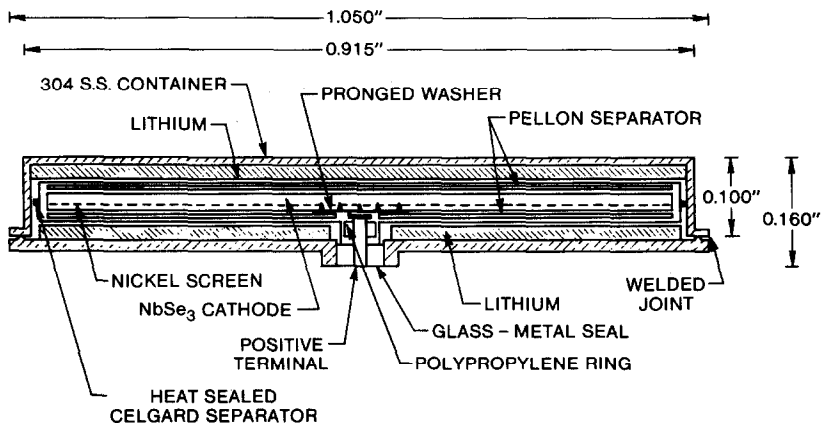
Fig. 2. Schematic drawing of the coin cell design involving a sandwich consisting of an NbSe₃ cathode between two lithium anodes. The can and header were the LTS-90 model from Exxon Enterprises. In a later design, the glass–metal seal was replaced with a ceramic–metal seal (Altus Corp.), and the flange was extended to site the resistance welding farther from the body of the cell. A few crimped seal cells were also constructed.

system were examined more extensively with larger cells containing a cathode of $NbSe_3$ pressed on a nickel screen sandwiched between two pure lithium anodes with both Celgard and Pellon polypropylene separators, as shown in Fig. 2. The theoretical capacities, based on 3 Li per $NbSe_3$, of these cells were generally 135 - 145 mA h, and cycling was typically between a charging limit of 2.5 - 2.8 V and a discharge cutoff of 1.05 V. At room temperature, we obtained as many as 32 cycles at 1 mA or 12 cycles at 5 mA discharge currents to a cutoff capacity of 100 mA h. At 60 °C, 19 cycles at 5 mA were obtained to the same cutoff capacity. The electrolyte solutions consisted of $LiAsF_6$ or LiI in either propylene carbonate or 2-methyltetrahydrofuran or in mixtures of these solvents.

In Fig. 3(a) we see discharge–charge curves for one of the better cells at different stages in its cycle life. The capacity as a function of cycle number for cells at different discharge currents and temperatures is shown in Fig. 3(b). These plots illustrate a typical precipitous drop in capacity at the end of life for the coin cells, attributable to the familiar failure of lithium anodes and/or electrolyte solution depletion, resulting from the accumulation of particulate lithium and film formation on cycling of lithium cells. This anode/electrolyte failure leaves the $NbSe_3$ cathode material capable of further cycling. Figure 3(c) shows discharge curves for a cell constructed using as the cathode material $NbSe_3$ which was recovered from "dead" coin cells. This demonstrates, at least, the feasibility of recycling used $NbSe_3$ and, perhaps, minimizing any environmental problems associated with disposal of $Li/NbSe_3$ cells. Figure 3(d) shows discharge–charge curves at 4 mA discharge and 2 mA charge for a cell in which the usual $NbSe_3$ loading of about 140 mA h was increased to give a theoretical capacity of 295 mA h. This cell
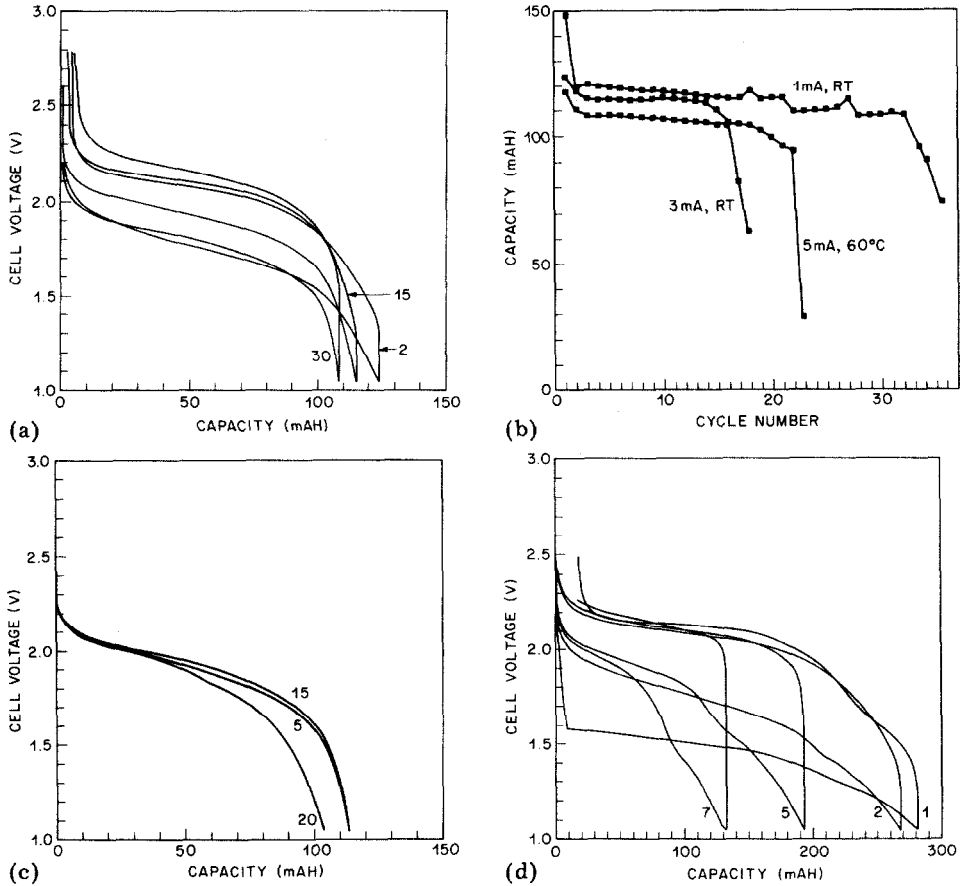
Fig. 3. (a) Discharge–charge curves at room temperature for the indicated cycle number for an Li/NbSe$_3$ coin cell discharged at 1 mA and charged at 0.5 mA. (b) Capacity $vs.$ cycle number for coin cells at the indicated discharge currents at room temperature and 60 °C. (c) Discharge curves at room temperature at the indicated cycle numbers for a cell constructed using NbSe$_3$ recovered from other cells which had been cycled to below the cutoff capacity of 100 mA h. (d) Discharge–charge curves for a cell heavily loaded with NbSe$_3$ to deliver more than the standard capacity and delivering 7 cycles to the 100 mA h cutoff capacity.

delivered 7 cycles to the 100 mA h cutoff. Two very heavily loaded cells only lasted 2 cycles, delivering 450 mA h on 1st discharge at 1 mA and 200 mA h on the 2nd discharge at room temperature. The coin cell effort was terminated at about this time and no optimization for increased cycle life in these high capacity cells was attempted.

A characteristic feature of Li/NbSe$_3$ cells, and lithium cells with other trichalcogenide cathodes, is the marked difference between the first discharge and succeeding discharge curves, as shown, $e.g.$ in Fig. 3(d). It is apparent that a fundamental change in the NbSe$_3$ takes place on lithiation that results in an increase in the voltage after the first discharge. Typically,
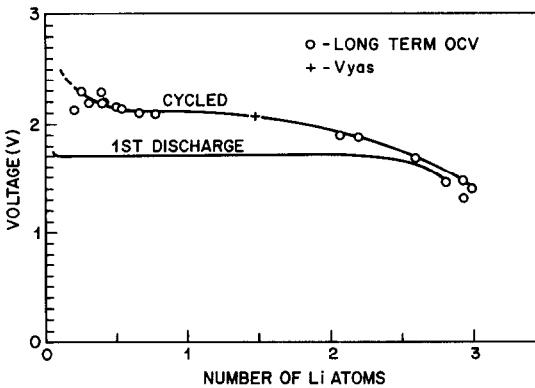
Fig. 4. "Equilibrium" open circuit voltage as a function of lithium insertion for 1st discharge [7] and for cycled Li/NbSe$_3$ cells. The curve was drawn to favor the data points corresponding to those coin cells stored for longer periods of time and showing no signs of leakage or internal shorting on storage. The mid-discharge point is from unpublished work of Vyas and represents an extrapolation of charge and discharge voltages at varying currents to zero current.

this increase in voltage continues for perhaps 5 - 15 cycles or so, as is evident in Fig. 3(a), 3(c) and, especially, in 3(d). Although the insertion of 3 lithiums into NbSe$_3$ resulted in material amorphous to X-rays in one study [2], a diffraction pattern indexed to NbSe$_3$ was reported in another paper [6]. The equilibrium open circuit voltage as a function of the amount of lithium insertion in virgin uncycled NbSe$_3$, i.e., on first discharge, has been published [7]. In order to obtain a similar equilibrium curve for the cycled material, a number of our well-behaved, cycled coin cells were stored on open circuit at various stages of charge or discharge for periods ranging from weeks to over 2 years. From the charge–discharge history of these cells, and from a mid-discharge point from unpublished work of Vyas, the approximate equilibrium discharge curve shown in Fig. 4 was obtained. The mid-discharge equilibrium voltage of slightly more than 2 V for the cycled cells is significantly higher than the equilibrium 1.7 V plateau for uncycled Li/NbSe$_3$ cells on 1st discharge [7]. The flat plateau in the initial discharge curve is suggestive of the formation of a second phase of Li$_2$NbSe$_3$, which might serve as the basic structure for further lithium insertion and extraction. Whatever the change in NbSe$_3$ on lithiation, it results in an obvious practical advantage over the uncycled NbSe$_3$ because of the resulting higher "theoretical" energy density (1.8 versus 1.6 W h cm^{-3}) on cycling. Of course, any need for a "formation" cycle or cycles adds to the cost of a commercial cell.

Cylindrical cells

The cylindrical AA cells utilized a jellyroll construction, as shown in Fig. 5. Again, pure lithium was used as the anode, Celgard as the separator,
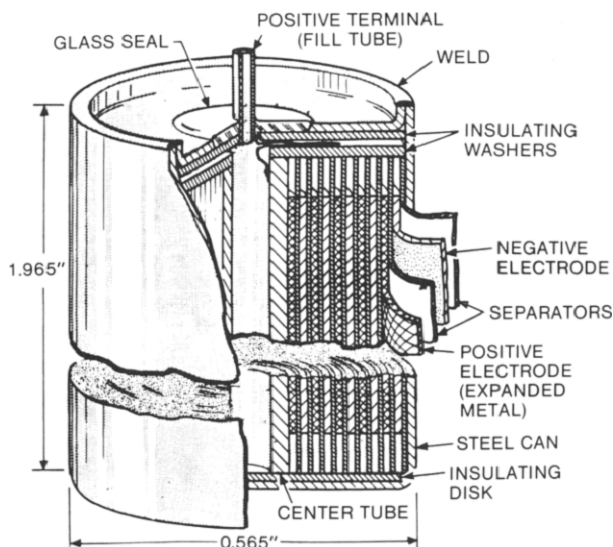
Fig. 5. Schematic drawing of the construction of the cylindrical Li/NbSe$_3$ AA cell.

and the cathode was prepared by rolling mats of fibrous NbSe$_3$ onto nickel expanded current collector. The flexibility of the NbSe$_3$ mats is such that a foil of pure NbSe$_3$ can be wadded up by hand and the crumpled material unfolded into its original shape and still maintain its integrity. One AA cell was even constructed without using any current collecting substrate for the cathode. The performance at higher currents was poor, as expected, but the cell was able to deliver over 700 mA h (50% of the theoretical) capacity at 30 mA.

The AA cylindrical cells typically contained sufficient NbSe$_3$ to deliver a theoretical capacity of about 1300 mA h on 1st discharge to 1 V. It has been found, however, that repeated cycling down to 1 V results in reduced cycle life, and our normal cycling routine involves charging to 2.4 V and discharging to 1.4 V, after one or two initial formation cycles discharging to 1 V. The rate capability of the AA cylindrical cells is illustrated in Fig. 6. Figure 6(a) shows the discharge curves at room temperature after 20 cycles for a number of different cells discharged at currents ranging from 80 to 1600 mA. It is seen that, even at the highest rate, the voltage remains above 1.6 V over most of the discharge, with mid-discharge voltages at the lower rates of up to 1.95 V, within 0.1 V of the mid-discharge equilibrium voltage in Fig. 4. Figure 6(b) shows more recent data for one particular cell cycled 20 times and then discharged at increasing currents up to 4 A in successive cycles. It is seen that at 3 A discharge current, a capacity of 800 mA h is delivered, while at 4 A discharge current, the capacity loss with increasing current is high, with the delivered capacity less than our normal 700 mA h cutoff limit, but still a respectable value of almost 600 mA h. The humps in the discharge curves at 3 and 4 A are most likely due to heating of the cell
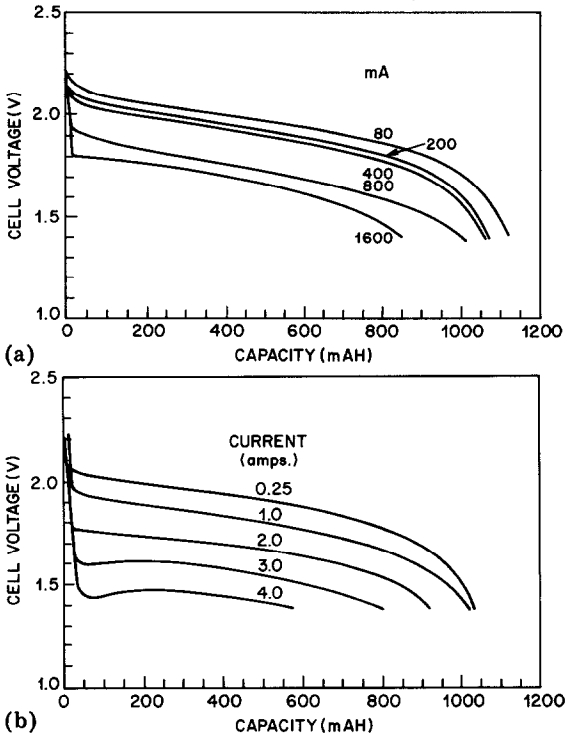
Fig. 6. (a) Discharge curves for a number of different cells discharged at the indicated currents at room temperature after 20 "standard" cycles. The standard cycles include 1 or 2 initial formation cycles discharging to 1 V, followed by cycling between 2.4 and 1.4 V at 400 and 80 mA discharge and charge currents, respectively. (b) The 21st - 25th discharge curves, with increased current in successive cycles, for a cell which had been cycled between 2.4 and 1.4 V at 400 mA and 120 mA discharge and charge currents, respectively, following 2 initial formation cycles. The charge current in the 21st - 25th cycles was 80 mA.

at these currents, resulting in higher electrolyte solution conductivities and lower iR drops.

The cycling behavior of one of the Li/NbSe$_3$ AA cells is shown in Fig. 7, which shows the discharge capacity as a function of cycle number for a cell cycled under the "standard" regime of 400 mA discharge and 80 mA charge currents. It is seen that the discharge capacity is relatively constant over about half the cycle life before any significant decay of cell capacity sets in. The decay in the capacity that follows is also relatively much more gradual than for the coin cells (see Fig. 3(b)). The best AA cell to date, cycling under the standard regime, has delivered 318 cycles to a cutoff capacity of 700 mA h. Discharge curves for this cell are shown in Fig. 8, which illustrates again the relatively slow decay in capacity over most of the cycle life.

The cycle life also depends on the charge rate, as would be expected from the less dendritic lithium morphologies at lower charge currents
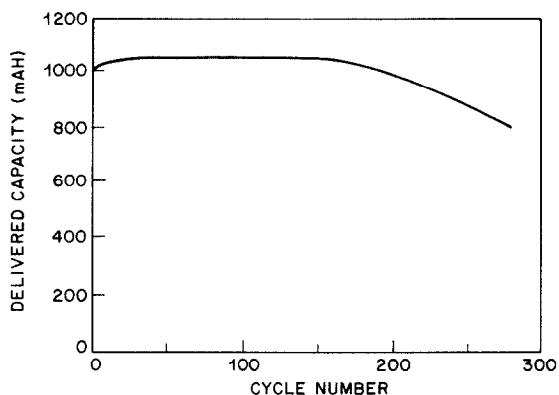
Fig. 7. Capacity *vs.* cycle number for a cylindrical Li/NbSe$_3$ AA cell cycling between 2.4 and 1.4 V at discharge and charge currents of 400 and 80 mA, respectively.
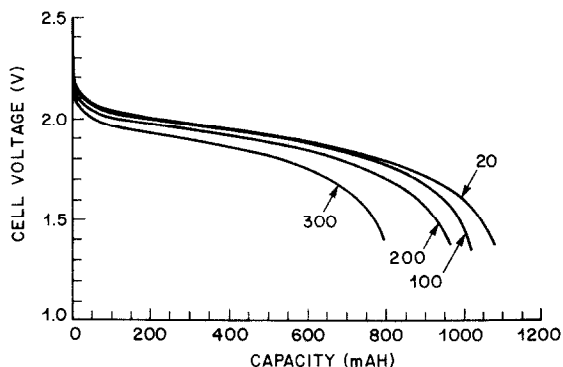

Fig. 8. Discharge curves for the indicated cycle numbers for one of the best cylindrical AA cells cycling between 2.4 and 1.4 V at discharge and charge currents of 400 and 80 mA, respectively.

(*e.g.*, see ref. 4). Any minimization of the formation of finely-divided dendritic lithium on cycling is also highly desirable from the safety standpoint, another reason to use as low a charging rate as possible consistent with the particular application. Charge currents of 80 - 120 mA are suitable for maintaining long cycle lives and are sufficiently high to permit practical charging times for most applications.

Another feature of most lithium cells *vis-a-vis* nickel/cadmium or lead/acid rechargeable batteries is the much lower self discharge rate of the lithium systems. The Li/NbSe$_3$ system is no exception and, indeed, seems to be especially suitable for long shelf life applications. Microcalorimetry data and storage tests on some AA cells indicate self discharge rates of about 1% per year for the AA cells at room temperature [8], as shown in Fig. 9, which also includes data at elevated temperatures. These results are also consistent with a few long term experiments in which cycled Li/NbSe$_3$ coin cells were
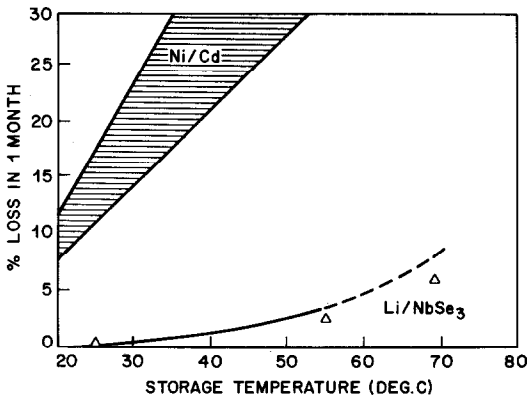
Fig. 9. Self-discharge behavior of Li/NbSe$_3$ AA cells as a function of temperature. The curve is based on microcalorimetric data from ref. 8, while the points are from storage tests on actual AA cells. Also shown is a range of self-discharge behaviors for typical Ni/Cd AA cells.
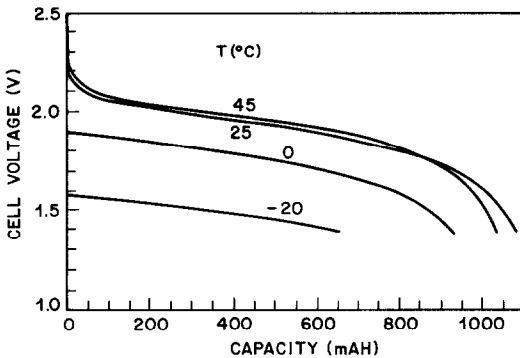
Fig. 10. Discharge curves for cells discharged at 200 mA at the indicated temperatures after 20 cycles at room temperature.

found to retain virtually all of their capacity after 2 - 3 years of open circuit storage at room temperature.

The effect of temperature on the performance of the Li/NbSe$_3$ AA cells is illustrated in Fig. 10, which shows discharge curves at 200 mA at temperatures between −20 and 45 °C. It is seen that over half the room temperature capacity is delivered at −20 °C.

In recent years, great strides have been made in extending the cycle life of lithium rechargeable batteries and in the construction of real cells of possible practical utility, as exemplified by the work here in the Vancouver area on the MOLICEL, with its MoS$_2$ cathode [9]. The increase in cycle life, however, does not come without presenting new challenges in the field of safety, particularly where larger high rate cells are concerned.

The behavior on electrical abuse of fresh and cycled 45 A h ("BC") MOLICELs has been reported and protective measures (diodes, heat sinking) to prevent the vigorous venting and flaming have been evaluated [10]. Our Li/NbSe$_3$ AA cells have generally been found to be quite resistant to various types of abuse, such as overcharge, reversal, shorting, etc., at least for lightly cycled cells (e.g., 20 cycles). Work is in progress to study and optimize the safety aspects of heavily cycled cells.

Conclusion

The performance of the Li/NbSe$_3$ AA cells in terms of energy density, rate capability, shelf life, and cycle life places the Li/NbSe$_3$ system in the forefront of rechargeable lithium technology. The energy density of over 300 W h l^{-1} for the AA cells in their standard construction is approximately 2.5 times that of nickel–cadmium AA cells. The power capability is shown in Fig. 11 along with that of Ni/Cd AA cells. The energy density in the Li/NbSe$_3$ AA cell can be made appreciably higher by packing in more NbSe$_3$ but we have not yet studied such cells to any significant extent. At any rate, the performance of the Li/NbSe$_3$ technology is now at a level of practical interest. The future of this, or any of the other lithium rechargeable technologies would seem to depend on demonstrating: (i) sufficient performance and economic advantages to compete with improving nickel/cadmium technology; (ii) a high level of safety for fresh and cycled cells/batteries.
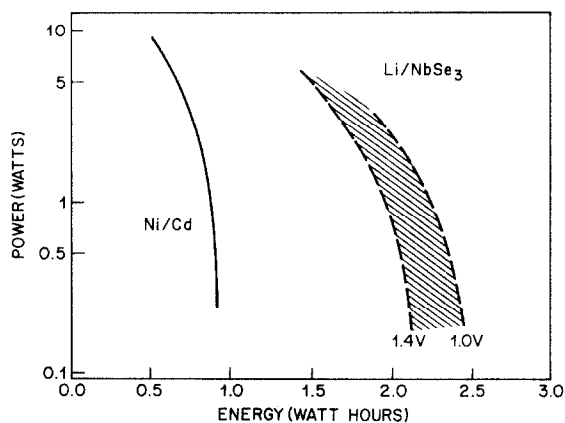

Fig. 11. Power vs. energy for Li/NbSe$_3$ and Ni/Cd AA cells. The shaded area for the Li/NbSe$_3$ cells covers the range between discharging to 1.0 and 1.4 V.

Acknowledgements

This paper is based on the results of a dedicated team effort on the AA cell by members of our Faraday team and on the coin cell by earlier

workers, all associated with the Battery Development Department. The rechargeable lithium effort has also benefited greatly from significant contributions by many members of the Research Area at AT&T Bell Labs and by workers at the AT&T Engineering Research Center.

References

1 J. Broadhead, F. J. DiSalvo and F. A. Trumbore, *U.S. Pat. 3,864,167* (1975); J. Broadhead and F. A. Trumbore, *Electrochem. Soc. Ext. Abstr., 73-1* (1973) 445; F. A. Trumbore and J. Broadhead, *Ext. Abstr., 73-1* (1973) 448; F. A. Trumbore, J. Broadhead and T. M. Putvinski, *Ext. Abstr., 73-2* (1973) 149.
2 D. W. Murphy and F. A. Trumbore, *J. Electrochem. Soc., 123* (1976) 960.
3 See, *e.g.*, D. W. Murphy and F. A. Trumbore, *J. Cryst. Growth, 39* (1977) 185.
4 J. Broadhead and F. A. Trumbore, in D. Collins, (ed.), *Power Sources 5*, Academic Press, London and New York, 1975, p. 661.
5 J. Broadhead, F. A. Trumbore and S. Basu, *J. Electroanal. Chem., 118* (1981) 241.
6 R. R. Chianelli and M. B. Dines, *Inorg. Chem., 14* (1975) 2417.
7 J. R. Carides and D. W. Murphy, *J. Electrochem. Soc., 124* (1977) 1309.
8 B. Vyas and Y. L. Barberio, unpublished results.
9 See, *e.g.*, J. A. Stiles, *J. Power Sources, 26* (1989) 233.
10 J. B. Taylor, D. Fouchard, D. Wainwright and L. Ruggier, *Proc. Electrochem. Soc., 87-16* (1987) 94.